Biosensors and Bioelectronics 143 (2019) 111607

Contents lists available at ScienceDirect

Biosensors and Bioelectronics

journal homepage: www.elsevier.com/locate/bios

A novel oriented antibody immobilization based voltammetric immunosensor for allergenic activity detection of lectin in kidney bean by using AuNPs-PEI-MWCNTs modified electrode

Xianbao Sun[a,1], Yongkang Ye[a,b,1], Shudong He[a,b,*], Zeyu Wu[a], Junyang Yue[a], Hanju Sun[a,b], Xiaodong Cao[a,b,**]

[a] School of Food and Biological Engineering, Engineering Research Center of Bio-process of Ministry of Education, Hefei University of Technology, Hefei, Anhui, 230009, PR China

[b] Anhui Province Key Laboratory of Functional Compound Seasoning, Anhui Qiangwang Seasoning Food Co., Ltd, Jieshou, Anhui, 236500, PR China

ARTICLE INFO

Keywords:
Voltammetric immunosensor
Allergenic activity detection
Kidney bean lectin
Oriented antibody immobilization
AuNPs-PEI-MWCNTs nanocomposite

ABSTRACT:

As a well-known allergenic indicator in kidney beans, lectins have always been the serious threats for human health. Herein, we introduced a new label-free voltammetric immunosensor for the direct determination of kidney bean lectin (KBL) with potential allergenic activity. Gold nanoparticles-polyethyleneimine-multiwalled carbon nanotubes nanocomposite was one-pot synthesized and modified onto the glass carbon electrode to enhance catalytic currents of oxygen reduction reaction. The KBL polyclonal antibody, acquired from rabbit immunization, was orientedly immobilized on the electrode modified with recombinant staphylococcal protein A via fragment crystallizable (Fc) region of antibody. Under the optimized condition, the immunosensor displayed a good linear response (R^2 = 0.978) to KBL with a range from 0.05 to 100 μg/mL and a detection limit of 0.023 μg/mL. Simultaneously, the immunosensor exhibited well selectivity, interference-resistant ability, stability (4 °C) and reproducibility. Compared with the conventional enzyme-linked immunosorbent assay (ELISA) method, the immunosensor was successfully applied to quantify allergenic activity of lectin in raw and cooked (boiled for 30 min) kidney bean milk samples. This new approach provides new perspectives both for rapid quantification of lectin in kidney beans-derived foodstuffs and as a real-time monitoring tool for the allergenic potential during the whole production and consumption process.

1. Introduction

Over the past decades, high culinary and industrial uses of kidney beans (*Phaseolus vulgaris*) have raised concerns to human health and wellness due to their potential toxic and allergenic reactions induced by the presence of lectins (He et al., 2018; Sun et al., 2019). Kidney bean lectins (KBLs) are the sugar-binding proteins that can resist to the degradation of heating and digestive enzymes, and then bind to the surface of epithelial cells to induce gastroenteritis, nausea, diarrhea, and even fatal reactions (Miyake et al., 2007; Vasconcelos and Oliveira, 2004). In 2006, more than 1000 people in Japan suffered from acute intestinal symptoms and 100 people were hospitalized, who tried the diet with roasted white kidney beans powder (Ogawa and Date, 2014). In China, 7526 individuals were poisoned by intake of KBL, which accounted for 40% of poisonous plants poisoning events from 2004 to 2013 (Sun et al., 2019). Although the safety guidelines have been recommended regarding kidney beans consumption (Kumar et al., 2013), fewer methods could be used for the rapid quantification and real-time monitoring of allergic potentials of lectin in kidney bean-derived foodstuffs, which would be in detriment to food consumption safety and health security.

In the previous studies, reverse phase HPLC (Adar et al., 1989), size-exclusion chromatography (Zhao et al., 2019), LC-MS/MS and PCR method (He et al., 2015) showed high sensitivity and accuracy in lectin detection, but these requiring instruments were much expensive and would not adapt to *in situ* and real-time analysis. In order to improve

* Corresponding author. School of Food and Biological Engineering, Engineering Research Center of Bio-process of Ministry of Education, Hefei University of Technology, Hefei, Anhui, 230009, PR China.

** Corresponding author. School of Food and Biological Engineering, Engineering Research Center of Bio-process of Ministry of Education, Hefei University of Technology, Hefei, Anhui, 230009, PR China.

E-mail addresses: shudong.he@hfut.edu.cn (S. He), xiaodongcao@hfut.edu.cn (X. Cao).

[1] Means co-first authors.

https://doi.org/10.1016/j.bios.2019.111607
Received 7 July 2019; Received in revised form 5 August 2019; Accepted 16 August 2019
Available online 17 August 2019
0956-5663/

the selectivity and precision, enzyme-linked immunosorbent assay (ELISA) has been successfully developed for plant lectin detection in traces of samples (Matucci et al., 2004; Vincenzi et al., 2002). Especially, the allergic potentials of lectins in native and/or processed foods could be successfully reflected by quantitative ELISA analysis, based on the high specificity of the molecular recognition between antibodies and antigens (Vincenzi et al., 2002; Zhao et al., 2019). However, the selection of labelled enzymes remained challenges to avoid tedious optimization steps and longer analysis time in the improvements of intrinsic spectroscopic properties (Singh et al., 2017). In this regard, electrochemical sensors have attracted more attentions due to the advantages of quick analysis, portability, high sensitivity, easy-to-operate, automation, and integration (Haghshenas et al., 2017; Li et al., 2017; Yu et al., 2013). Based on carbohydrate–lectin interaction specificity, sugars were immobilized on electrochemical platforms for specific recognition and fast response to lectin, such as mannose/glucose *vs.* Concanavalin A (Con A) (Casas-Solvas et al., 2008; Loaiza et al., 2011; Min et al., 2010) and lactose/mannose *vs. Lens culinaris* lectin (Szunerits et al., 2010). Although high sensitivity and low limit of detection (LOD) were established in sugar-binding lectin detection, the allergenicity potential could not be analyzed by the results. Then it seems to be interesting to develop an electrochemical immunosensor by combining the high selectivity of the immunoassays with high sensitivity of electrochemical methods. However, to the best of our knowledge, no related information has been well documented, and appropriate designs for the allergenic lectin detection in the processed foods have not been attained yet.

In order to enhance analytical performances, various nanomaterials have been utilized for the construction of electrochemical immunosensors. Gold nanoparticles (AuNPs) is one of the most widely-used nanomaterials due to its large specific surface area, high surface free energy, good conductivity and biocompatibility (Huang et al., 2010; Jie et al., 2014). It has been suggested that the adsorbed proteins on the colloidal gold nanoparticles could retain their bioactivity (Crumbliss et al., 1992). Multi-wall carbon nanotubes (MWCNTs) consisting of up to several tens of graphitic shells have caught our full attentions as showing high aspect ratio, nanometer sized dimensions, good electrical conductivity, and strong adsorption properties (Liu et al., 2017; Yuan et al., 2014). However, MWCNTs would form large bundles in water due to strong van der Waals interactions, which limited further application in designing biosensors (Wu et al., 2017). Then, due to extraordinary water-solubility, polyelectrolytes, such as polyethyleneimine (PEI), could be used to serve as dispersers and stabilizers to protect the MWCNTs from aggregating (Jin et al., 2013; Wu et al., 2017). Immobilization of antibodies would be another vital step in the fabrication of immunosensor (Jie et al., 2014). Although many immobilization techniques have been developed mainly based on the physical, covalent, and bio-affinity immobilization mechanisms in the past years (Skottrup et al., 2008), partial or complete loss of protein activity might happen during the immobilization, due to random orientation and steric-hindrance (Afkhami et al., 2017; Tang et al., 2006). Scanning from the antibody (Ab) purification strategies (Ey et al., 1978; Miller and Stone, 1978), the absorbent of immunoglobulin-binding Staphylococcal protein A (SPA) could be one of the best candidates for oriented immobilization of antibodies, which includes a signaling sequence (Abrahmsén et al., 1985), a C-terminal anchoring part (Moks et al., 1986), and an IgG-binding region consisting of five highly homologous domains, that can selectively bind the Fc fragment of the Ab leaving the fragment of antigen binding (Fab) available for antigen detection (Moks et al., 1986). SPA was once used as an immunological probe in the cell surface markers analysis (Dorval et al., 1974). Recently, SPA-mediated oriented antibody immobilization has been applied in the immunosensors, and remarkably improved detection performance because of the effective exposures of Ab molecules to antigen interactions (Jie et al., 2014; Kausaite-Minkstimiene et al., 2010; Malvano et al., 2016).

Herein, we describe a novel label-free voltammetric immunosensor for sensitive detection of allergenic KBL. The KBL Ab was prepared and evaluated in our preliminary experiments. In order to amplify current signals, one-pot synthesized AuNPs-PEI-MWCNTs nanocomposite, by employing PEI as a difunctional agent both for improving the dispersibility of MWCNTs, and as a reductant for *in situ* forming AuNPs onto MWCNTs, was used to modify glassy carbon electrode (GCE). Subsequently, recombinant SPA with additional cysteine residue (SPA-Cys) was immobilized onto modified electrode via strong interaction of the thiol group with the AuNPs surface for oriented Ab immobilization. Finally, the analytical performance of the fabricated immunosensor for allergenic KBL was performed. Compared to sugar-mediated sensors and ELISA, this new approach provided a time-saving, sensitive, and allergenicity-recognizable detection for lectin regarding to the safety consumption of kidney beans-derived foodstuffs.

2. Material and methods

2.1. Reagents and apparatus

KBL standard (from red kidney bean), Concanavalin A (Con A), bovine serum albumin (BSA), γ-globulin (from bovine blood), polyethyleneimine (PEI, branched, average Mw ~25,000), chloroauric acid ($HAuCl_4$) were purchased from Sigma Chemical Co., Ltd (St. Louis, MO, USA). Black turtle bean lectin was purified according to our previous studies (He et al., 2015; Zhao et al., 2019). Recombinant SPA-Cys was purchased from Shanghai Yaxin Biotechnology Co., Ltd. (Shanghai, China). Carboxyl functionalized MWCNTs was obtained from Nanjing Xianfeng nano Co. (Nanjing, China). Other chemicals employed in the study were analytical reagent grade.

UV–vis absorption spectra were recorded on a UV-4802 spectrophotometer (Unico Shanghai Instrument Co., Ltd. Shanghai, China). The morphology and size of the nanomaterials were analyzed with a Tecnai G2 transmission electron microscope (TEM, FEI, Netherlands, at an accelerate voltage of 200 kV). Electrochemical measurements were performed on a CHI 660D electrochemical workstation (Chenhua Corp., Shanghai, China) with a standard three-electrode configuration (Fig. S1). A Pt wire provided the counter electrode, an Ag/AgCl electrode acted as the reference, and a modified glassy carbon electrode (GCE, 3 mm in diameter) was used as the working electrode.

2.2. Preparation of the Ab

The KBL polyclone Ab was acquired from rabbit immunization by KBL standard antigen. The KBL protein (0.5 mg) with complete Ferund's adjuvant was injected subcutaneously into the back of rabbits. After 2 weeks, booster immunization was proceed by injecting KBL with incomplete Ferund's adjuvant with one week intervals. The sera were collected after four booster immunization injections, and anti-KBL IgG was purified by protein G-sepharose 4B fast flow column. The titer evaluation of Ab was analyzed by ELISA according to Afkhami's method (Afkhami et al., 2017). Briefly, KBL protein (10 μg/mL, in carbonate-bicarbonate buffer) was coated on ELISA plate with 60 min incubation at 37 °C, and then was blocked with BSA (2%, in PBST). Afterwards, the plate was incubated with a serial dilution of rabbit anti-KBL IgG (500 ng–1 ng, in PBST) for 60 min at 37 °C, followed by incubation with goat anti-rabbit IgG conjugated with horseradish peroxidase (1:4000 dilution, in PBST). The end of each step was washed with PBST for 3 times at least. Finally, a 100 μL of O-phenyldiamine substrates (in citrate-phosphate buffer) was added to each well for 20 min in the dark. After stopping the reaction with sulfuric acid (2M), the plate was read at 492 nm by using an ELISA reader. The above procedures were delegated to Nanjing SenBeiJia Biological Technology Co., Ltd. (Nanjing, Jiangsu, China). Finally, the obtained Ab was supplied as a liquid in PBS (10 mM, pH 7.4) with a concentration of 1.0 mg/mL (lot specific).

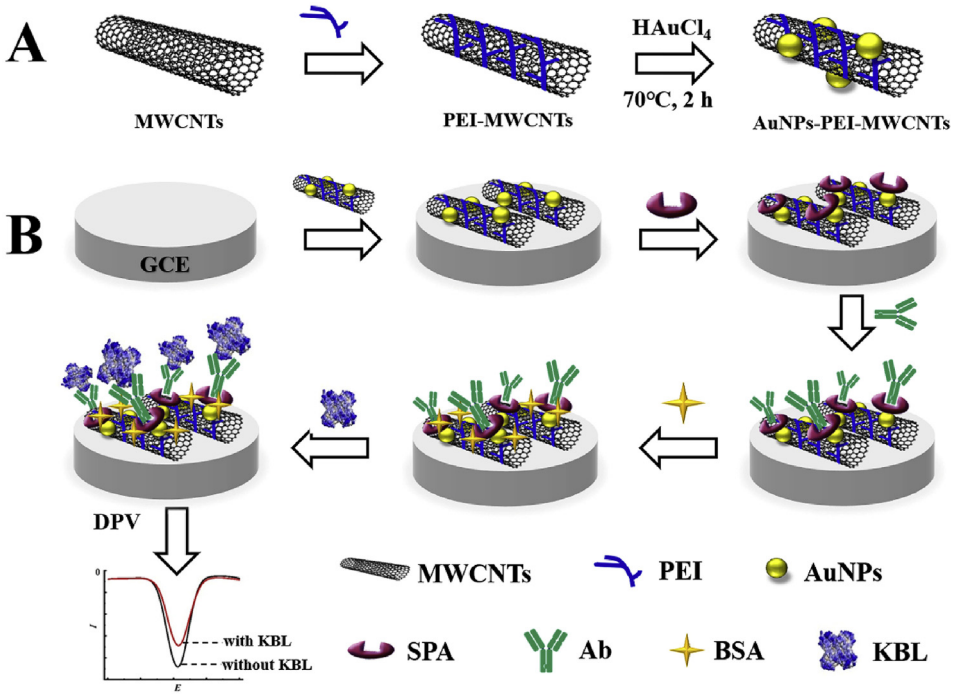

Scheme 1. Schematic illustration for (A) synthesis of AuNPs/MWNT/PEI nanocomposite, (B) fabrication steps of the immunosensor for the determination of KBL.

2.3. One-pot synthesis of AuNPs-PEI-MWCNTs nanocomposite

Two milligram MWCNTs and 50 mg PEI were dispersed in 8 mL ultrapure water by ultrasonic agitation for 30 min. Subsequently, 2 mL $HAuCl_4$ (10 mg/mL) was mixed into the dispersion and heated at 70 °C for 2 h. After centrifugation (14000 rpm, 10 min) and washing at least three times to move away redundant PEI and AuNPs. The final sediment was dispersed in distilled water to obtain the AuNPs-PEI-MWCNTs composite. The synthesis scheme is shown Scheme 1A.

2.4. Fabrication of the immunosensor

Before modification, the bare GCE was polished with Al_2O_3 (0.3 and 0.05 μm) slurry, followed by washing with distilled water and sonicating in ethanol, distilled water, respectively. After drying at room temperature, 5 μL prepared AuNPs-PEI-MWCNTs composite solution (2 mg/mL) was drop coated onto the cleared GCE surface. Next, 10 μL SPA-Cys (2 mg/mL in 10 mM PBS, pH 7.4) was dropped onto the electrode and was immobilized for 2 h. Afterwards, 5 μL Ab (0.15 mg/mL in 10 mM PBS, pH 7.4) was dropped onto the SPA-Cys modified electrode for a 90 min incubation at 37 °C. At last, the electrode surface was blocked by BSA (1% w/v) for 1 h to eliminate the possible active sites and prevent non-specific binding. After each modification step, the electrode was rinsed thoroughly by the PBS (10 mM, pH 7.4) to remove the unbound/weak-bound molecules until the measurement signal was stable and repeatable. The fabrication process of the immunosensor is illustrated in Scheme 1B.

2.5. Electrochemical measurements

All the electrochemical measurements were performed in PBS (10 mM, pH 7.4) containing 0.1 M KCl and 5 mM $K_3Fe(CN)_6/K_4Fe(CN)_6$ redox pair. Electrochemistry characterization of immunosensor fabrication was performed using cyclic voltammetry (CV) at scanning rate of 100 mVs^{-1} from −0.2–0.6 V. Differential pulse voltammetry (DPV) technique was employed for the response studies of samples detection, recorded at a potential from −0.1 to 0.5 V with pulse amplitude 50 mV, pulse period 0.5 s, and pulse width 50 ms, respectively. Prior to detection, 10 μL of samples were dropped onto the fabricated KBL-immunosensors and incubated at 37 °C for 60 min to form the immunocomplex between Ab and KBL. The DPV the oxidation peak currents (I_{sample}) were then recorded after the electrodes were washed thoroughly with PBS to remove any residue and loosely bound KBL. The current of immunosensor treated with PBS was used as the blank (I_0), and thus the KBL detection result was finally based on the current difference (ΔI, $\Delta I = I_{sample}$-I_0) of two DPV measurements. All electrochemical measurements were carried out at room temperature (25 °C).

2.6. Preparation and analysis of kidney bean milks

To evaluate allergenicity-recognizable capacity of the immunosensor in the practical application, raw and cooked (boiled for 30 min) kidney bean milks were prepared, respectively. The milk samples were centrifuged at 8000 rpm for 10 min at 4 °C, and the clear supernatants were finally diluted to 5000 × (1:5000 w/v) in PBS (10 mM, pH 7.4), and the DPV responses were recorded as previously described. The recovery test was carried out by KBL standard addition with designated concentrations.

Quantitative ELISA method as described previously (Matucci et al., 2004; Simone et al., 2002) was utilized for the comparison to the immunosensor. Firstly, 96-well flat-bottomed microtiter plates were coated with 50 μL of ovalbumin (20 μg/mL) in 50 mM Na-carbonate buffer (pH 9.6) and incubated for 4 h at 37 °C. Afterwards, 50 μL lectin samples were added and incubated at 37 °C for 1 h, followed by successively incubating with 50 μL of the Ab (diluted 1:2000 in PBS-BSA) and 50 μL of AP-labelled monoclonal anti-rabbit IgG antibody ($AP\text{-}Ab_2$, obtained from Nanjing SenBeiJia Biological Technology Co., Ltd., Nanjing, Jiangsu, China, diluted 1:5000 in PBS-BSA). After each step, the plates were washed with PBS, blocked with 1% BSA for 30 min, and washed with PBS, respectively. Seventy-five microliters of alkaline phosphatase substrate (Sigma Fast p-nitrophenyl phosphate) was finally added to each well. The optical density (OD value) was measured at 450 nm within 30 min by a Microplate Reader (Tecan Infinite 200Pro, Tecan Group Ltd., Mannedorf, Switzerland). The calibration curve was obtained using KBL standard with the concentrations of 10–1000 ng/mL.

2.7. Statistical analysis

Data are expressed as mean ± standard deviation (SD). Analyses of variance (ANOVA) with a significance level of 0.05 and the values of RSD were calculated using SPSS version 11.5 (SPSS Inc. Chicago, IL, USA).

3. Results and discussion

3.1. Availability evaluation of prepared Ab

Although KBL polyclonal Ab was successfully prepared, the availability for electrochemistry detection, including binding capacity, specificity, and allergenicity-recognizable ability of prepared Ab to KBL, need to be evaluated, since it would be the important precondition for our immunosensor development. Thus, in the preliminary investigation, a simple BSA/Ab/AuNPs/GCE sensor was assembled by directly electrodeposition AuNPs onto GCE to adsorb Ab. Then, a series of detections for (a) 0, 0.1 and 10 μg/mL of KBL; (b) 10 μg/mL of KBL, Con A, and BSA; (c) 10 μg/mL of raw and cooked KBL were carried out. The Ab modified electrode with 0.1 μg/mL of KBL produced lower DPV signal than the sample without KBL, and a further decrease could be observed with 10 μg/mL of KBL (Supplementary Fig. S2A). Compared with interfering proteins including Con A and BSA, the electrode exhibited a more significant decrease in peak current (Fig. S2B), suggesting the concentration-dependent binding capacity and specificity of the prepared Ab to KBL. Since cooked KBL lost allergic activity, it should be noteworthy that the signal of cooked sample of 10 μg/mL was far less than that of raw KBL (Fig. S2C), even less than 0.1 μg/mL of KBL, indicating a well allergenicity-recognizable capacity of the prepared Ab. A comparison of DPV peak current differences (ΔI) was also shown in Fig. S2D, which confirmed that the prepared Ab was available for further immunosensor design.

3.2. Construction and characterization of the immunosensor

To improve the performance of the immunosensor, AuNPs-PEI-MWCNTs nanocomposite was synthesized for signal enhancement of the electrodes. Carboxylated MWCNTs were selected as supporting materials to improve electronic conductivity and chemical stability. As shown in Fig. 1A(a), since MWCNTs was easily aggregated even suffering a long-time stirring and ultrasonication, amino-rich PEI (branched), an amino-rich cationic polyelectrolyte, was closely coated onto MWCNTs as a disperser to improve the stability and homogeneity due to its good water-solubility (Fig. 1A(b)). PEI could combine with MWCNTS by virtue of electrostatic interaction and the formation of covalent bond between amino and carboxyl groups (Cao et al., 2011), besides, amines also have high affinity for physisorption along the carbon nanotubes sidewalls (Muñoz et al., 2005; Hu et al., 2006). In addition, PEI has a high density of amino-groups and a more branched structure, which could serve as primers and the reducing agent for the adsorbing anionic $AuCl^{4-}$ and then reducing to AuNPs (Hu et al., 2006), which *in situ* formed on the surface of MWCNTs. Due to efficient AuNPs-PEI-MWCNTs interaction, as shown in Fig. 1A(c), the stability of the composites would be improved greatly.

As presented in the UV–vis absorption spectra of MWCNTs, PEI, AuNPs-PEI, and AuNPs-PEI-MWCNTs (Fig. 1B), the obvious absorption peak at 525.5 nm in curves of AuNPs-PEI or AuNPs-PEI-MWCNTs composites would be attributed to the characteristic absorption of AuNPs (Huang et al., 2010), which was in agreement with the color changing to black/deep wine red (Fig. 1A(c)). Also, the diameter of ~10 nm for MWCNTs (Fig. 1C) was observed by using TEM, and Fig. 1D clearly showed that the *in situ* formed AuNPs were bonded closely on the surface of MWCNTs with a particle size of ~5–20 nm. Few AuNPs could be found on other regions without MWCNTs, indicating that free AuNPs that did not attach onto the MWCNTs surface have been removed. The AuNPs-PEI-MWCNTs nanocomposite showed good stability as no obvious morphology change could be observed after storing 4 weeks (Fig. S3). We further employed CV measurements (in 5 mM $[Fe(CN)_6]^{3/4-}$) to contrast the electrochemical behaviors of MWCNTs, PEI-MWCNTs, and AuNPs-PEI-MWCNTs modified GCE. As expected, the peak current of AuNPs-PEI-MWCNTs modified electrode (curve c, Fig. 2A) was higher than those of the MWCNTs (curve a) and PEI-MWCNTs (curve b). Therefore, these results proved that the composites were well prepared for signal amplification. Due to physical sorption and strong interaction of the thiol group with AuNPs, recombinant SPA-Cys was subsequently bond onto the surface of AuNPs-PEI-MWCNTs layer. Thus, it was expected that the Ab could be well-oriented on the surface of SPA coating and interact well with KBL.

The electrochemical characterizations of fabrication steps of the immunosensor were also further monitored by CV measurements. As shown in Fig. 2B, a reversible couple of well-defined redox peaks was observed in the bare GCE curve (curve a), owing to oxidation and reduction of $Fe(CN)_6^{3-}$ and $Fe(CN)_6^{4-}$, respectively. These peak currents remarkably increased upon modification with AuNPs-PEI-MWCNTs composite as displayed in curve b, indicating the significant facilitation of the electron transfer of Fe^{3+}/Fe^{2+} that could be attributed to high electronic conductivity of MWCNTs and AuNPs. However, addition of SPA caused a decrease in these current peaks (curve c) due to steric hindrance effect from the non-conductive SPA. Further decrease in peak currents was observed after Ab immobilizing (curve d) and BSA blocking (curve e), suggesting successful immobilization of Ab and adsorption of BSA onto the electrode. As expected, when the electrode was incubated with KBL, an obvious decrease of redox peak current was observed (curve f, Fig. 2B) as a result of Ab-KBL immunocomplex structures formed on the immunosensor, which acted as the inert electron and mass transfer blocking layer and it hindered the diffusion of ferricyanide toward the electrode surface (Huang et al., 2010). The conformational changes of protein caused by Ab-antigen interaction could also affect electron transfer and thus lead to the changes of redox peak current (Eissa et al., 2012). As a result, we can conclude that the proposed immunosensor was fabricated successfully.

3.3. Optimization of analytical conditions

In order to achieve the best sensitivity of KBL detection, the several analytical parameters were optimized using DPV measurements (in 5 mM $[Fe(CN)_6]^{3/4-}$). Respective variation (ΔI) of response current are given in the Supporting Information, Fig. S4. For MWCNTs concentration, as shown in Fig. S4A, the ΔI increased from 1.0 to 2.0 mg/mL, with a maximum of 13.55 μA at 2.0 mg/mL. The temperature 25 °C was selected in SPA immobilization due to the highest variation of catalytic peak current (Fig. S4B). Then the effects of incubating concentration (0.01–0.2 mg/mL) and temperature (4–45 °C) on antibody immobilization were investigated. As shown in Fig. S4C, when the concentration of Ab was over 0.15 μg/mL, the ΔI did not rise, indicating the active Ab-binding sites of SPA had reached a maximum binding capacity to Ab. Fig. S4D showed a gradual increase of ΔI from 4 to 45 °C. Because high temperature (45 °C) may damage the structure of proteins leading to the instability of ΔI signals, the practical operating Ab incubation temperature for the immunosensor was chosen to be 37 °C. Antigen-antibody immunoreaction have direct effects on the response sensitivity of the fabricated immunosensor. As depicted in Fig. S4E and F, 60 min at a temperature of 37 °C for KBL incubation have the maximum current responses of immunoreaction. Besides, the pH 5.0–9.0 of the buffer solution were studied (Fig. S4G). The ΔI value increased with pH from 5.0 to 7.4, and then decreased from 7.4 to 9.0, thus we finally choose detection buffer with pH 7.4 in the following tests.

3.4. Analytical performance of the immunosensor

To examine the analytical performance of the constructed

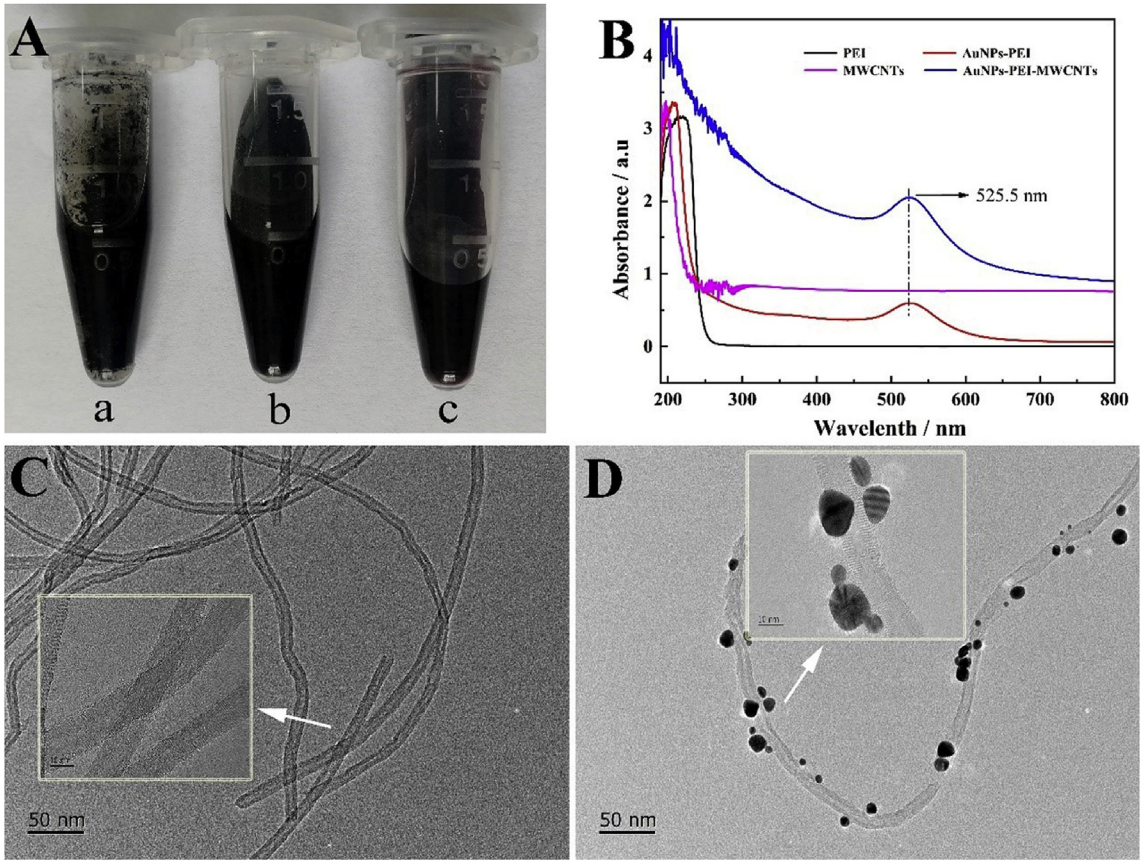

Fig. 1. Characterization of the nanocomposite. (A) The Photos of MWCNTs (a), PEI-MWCNTs (b), and AuNPs-PEI-MWCNTs (c), dispersed in distilled water with the concentration of 2 mg/mL (with MWCNTs as concentration calculation). (B) UV–vis of PEI, AuNPs-PEI, MWCNTs, and AuNPs-PEI-MWCNTs. (C) TEM image of MWCNTs. (D) TEM image of AuNPs-PEI-MWCNTs.

immunosensor, different concentrations of KBL standard (from 0.05 to 100 μg/mL) were used for DPV measurement under optimized conditions for the fabricated immunosensor, employing $[Fe(CN)_6]^{3/4-}$ as electron mediator. Experimental DPV dose-response curve (Fig. 2C) showed corresponding signal decreased with increasing concentration of KBL in the presence of (a) 0 μg/mL, (b) 0.05 μg/mL, (c) 0.2 μg/mL, (d) 1.0 μg/mL, (e) 5.0 μg/mL, (f) 10 μg/mL, (g) 50 μg/mL, and (h) 100 μg/mL, which might due to the formation of Ab-KBL immunocomplex that served as an insulating layer and repulsive electrostatic interaction between $Fe(CN)_6]^{3/4-}$ and antigen (Yang et al., 2014), and the data were in agreement with previous results of CV (curves e and f, Fig. 2B). As seen from the inset in Fig. 2D, due to the saturation binding of Ab-KBL, the ΔI would tend to be stable in the high concentration range of KBL. Calibration plot (Fig. 2D) displayed a positive linear relationship between ΔI and lg KBL concentration (lg C) from 0.05 to 100 μg/mL. The regression equation was $\Delta I = 17.429 \lg C + 27.14$, with the correlation coefficient of $R^2 = 0.978$ (n = 3). The limit of detection (LOD) was calculated as 0.023 based on the statistical approach (S/N = 3) according to the previous reports (Ye et al., 2018, 2019). As shown in Table 1, the performance of the developed immunosensor versus with available methods for plant lectins were compared. The new designed immunosensor showed a significantly improved linear range compared with conventional ELISA assays (125–500 ng/mL for wheat germ lectin, 250–1000 ng/mL for Con A) (Vincenzi et al., 2002), surface plasmon resonance (1.0–20 μg/mL for Con A) (Huang et al., 2013), carbohydrate-modified electrochemical sensor (0.1–1 μM for *Lens culinaris* lectin) (Szunerits et al., 2010), ECL biosensor (0.190–10 μg/mL for Con A) (Kwon et al., 2018), quartz crystal monitor (0.5–4.5 nM for Con A) (Zeng et al., 2014), and fluorescence biosensor (0.2–192.5 nM for Con A) (Liu et al., 2016). Furthermore, the immunosensor exhibited a lower limit of detection than the previous studies listed in Table 1. Compared with the ΔI obtained by BSA/Ab/AuNPs/GCE sensor in the preliminary experiment, the new designed BSA/Ab/SPA/AuNPs-PEI-MWCNTs/GCE immunosensor exhibited a higher sensitivity, as the ΔI of 10 μg/mL KBL was 46.7 μA by using new designed immunosensor, considerably higher than 12.1 μA obtained by BSA/Ab/AuNPs/GCE sensor. The reason could be partly attributed to that the large surface area of the AuNPs-PEI-MWCNTs-modified GCE platform has low background current and rich surface chemistry (Uslu and Ozkan, 2007), and enhanced catalytic currents (~200% in CV, Fig. 2B) improved by the AuNPs and MWCNTs presented in the AuNPs-PEI-MWCNTs nanocomposite. Furthermore, SPA onto modified GCE could specifically bind to the heavy chains on the Fc region of Ab, and effectively orient the interacting sites (Fab) of Ab to the test solution and interact well with KBL molecules (Jie et al., 2014; Malvano et al., 2016), also leading to a higher sensitivity. Additionally, $[Fe(CN)_6]^{3-/4-}$ is an excellent redox mediator in the electrochemical system that produced stable current with lower background noise (Yang et al., 2014).

3.5. Selectivity, interference-resistant ability, reproducibility and stability of the immunosensor

Practical detection system often consists of various substances that may interfere precision. Here, selectivity performance of the immunosensor was evaluated by using 1.0 μg/mL of KBL against black turtle bean lectin, Con A, BSA, and γ-globulin. As shown in Fig. 3A, the ΔI of interfering proteins including Con A, BSA and γ-globulin was less than 5 μA, much lower than 20.3 μA of KBL. It was noticeable that the immunosensor showed a relatively high ΔI signal (16.8 μA) when

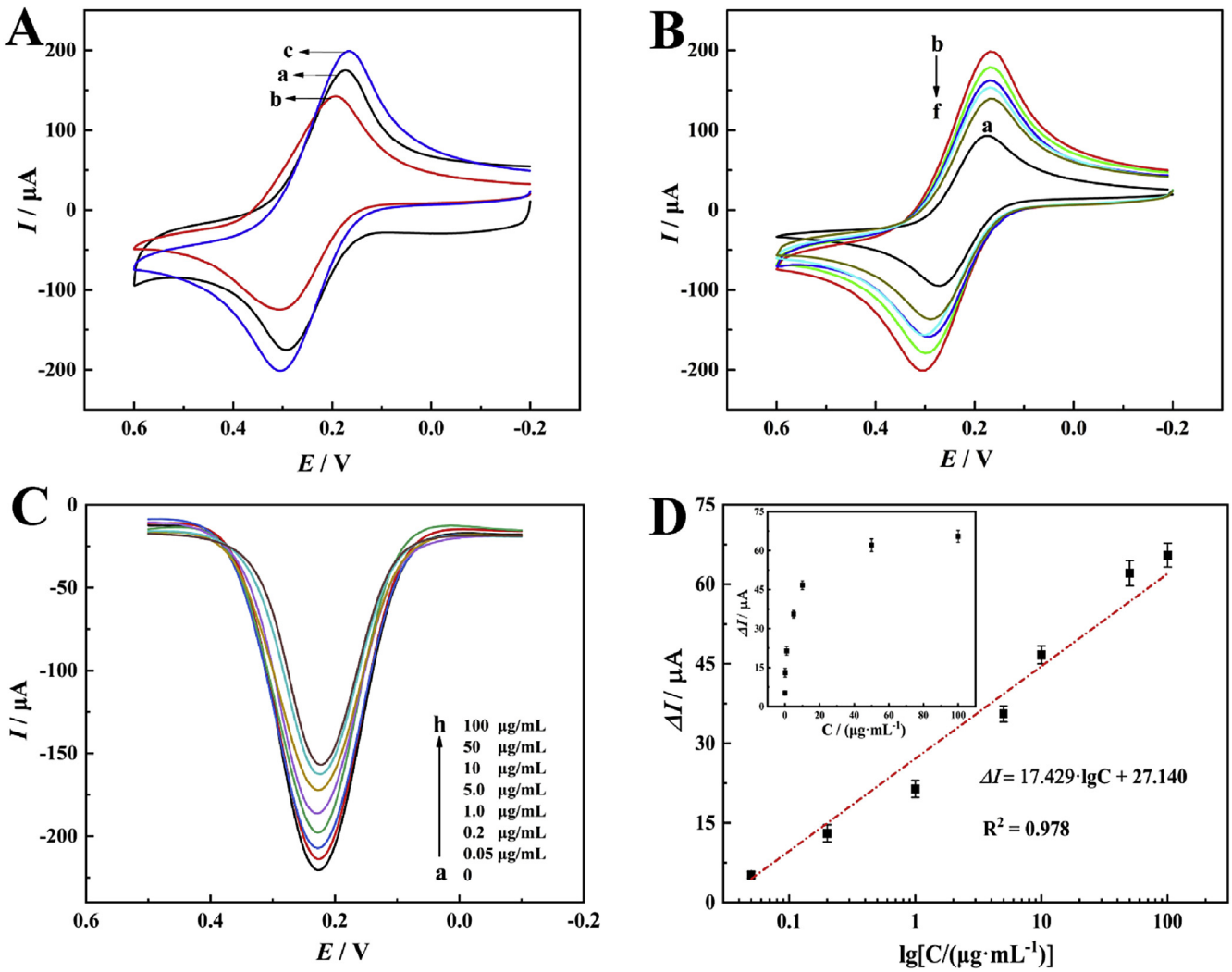

Fig. 2. CV curves (A) of MWCNTs/GCE (a), PEI-MWCNTs/GCE (b), and AuNPs-PEI-MWCNTs/GCE (c); CV curves (B) of bare GCE (a), AuNPs-PEI-MWCNTs/GCE (b), SPA/AuNPs-PEI-MWCNTs/GCE (c), Ab/SPA/AuNPs-PEI-MWCNTs/GCE (d), BSA/Ab/SPA/AuNPs-PEI-MWCNTs/GCE (e), KBL/BSA/Ab/SPA/AuNPs-PEI-MWCNTs/GCE (f); (C) DPV responses for KBL standard with the concentration of 0, 0.05, 0.2, 1.0, 5.0, 10, 50, and 100 μg/mL, in 5 mM $[Fe(CN)_6]^{3-/4-}$ solution (pH 7.4, containing 10 mM KCl) at scan-ning rate of 100 mVs-1; (D) Corresponding calibration curve (lgC vs ΔI) of immunosensors recorded for 0.05–100 μg/mL KBL, the inset shows the curve of the currents against the KBL concentrations, error bars represent standard deviation, $n = 3$.

Table 1
Comparison of analytical properties of different methods for the detection of plant lectins.

Methods	Linear range	Detection limit	Samples	Ref.
Microtiter plate	–	5 μg/mL	*Ricinus communis* lectin/Con A/wheat germ lectin	Hatakeyama et al. (1996)
ELISA	125–500 ng/mL	30 ng/mL	wheat germ lectin	Vincenzi et al. (2002)
ELISA	250–1000 ng/mL	80 ng/mL	Con A	Vincenzi et al. (2002)
Surface plasmon resonance	1.0–20 μg/mL	0.39 μg/mL	Con A	Huang et al. (2013)
Fluorescence resonance energy transfer	0.2–200 μg/mL	0.0747 μg/mL	Con A	Lim et al. (2012)
Electrochemical sensor	0.1–1 μM	5 nM	*Lens culinaris* lectin (MW ~ = 92 kDa)	Szunerits et al. (2010)
Quartz crystal monitor	0.5–4.5 nM	–	Con A	Zeng et al. (2014)
ECL biosensor	0.190–10 μg/mL	0.146 μg/mL	Con A	Kwon et al. (2018)
Fluorescence biosensor	0.2–192.5 nM	0.08 nM	Con A ((MW ~ = 104 kDa))	Liu et al. (2016)
Electrochemical immunosensor	0.05–100 μg/mL	0.023 μg/mL	KBL	This work

incubated with black turtle bean lectin, which due to a high homology (98.18% similarity) in amino acid sequence (He et al., 2015), implied that the immunosensor might be extended to other *Phaseolus vulgaris* lectins. Furthermore, as presented in Fig. 3A, KBL (1.0 μg/mL) mixed with 10 times higher concentration of the interferences (Con A, BSA, and γ-globulin) displayed the similar signal values ($P > 0.05$) to that of only KBL. Therefore, this study validated that the fabricated immunosensor was highly selective, specific and interference-resistant.

Furthermore, five working immunosensors were fabricated independently under the same condition to evaluate reproducibility by using KBL at the concentration of 1.0 μg/mL, and an acceptable relative standard deviation (RSD) of 2.24% was obtained (Fig. 3B). The stability of the prepared immunosensor was inspected after 0, 2, 4, 8 and 15 days by keeping the electrodes at 4 °C. As shown in Fig. 3C, the ΔI of the immunosensor showed small differences after 0, 2, and 4 days, with a minor change < 10%, and the response retained 86.45% and 71.36% of

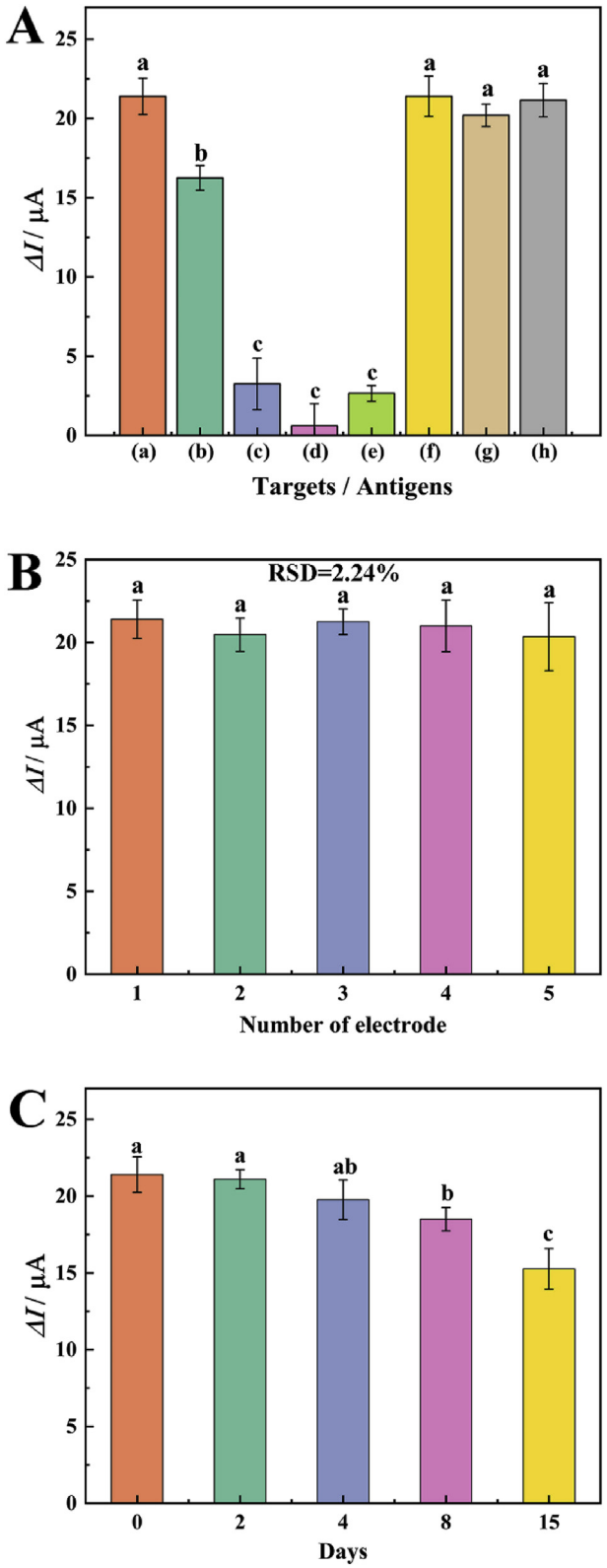

Fig. 3. DPV peak current change (ΔI), in 5 mM $[Fe(CN)_6]^{3-/4-}$ solution (pH 7.4, containing 10 mM KCl), for (A) interference study of the immunosensor towards 1.0 μg/mL KBL (a), 1.0 μg/mL black turtle bean lectin (b), 1.0 μg/mL Con A (c), 1.0 μg/mL BSA (d), 1.0 μg/mL γ-globulin (e), and 1.0 μg/mL KBL mixed with 10 μg/mL Con A (f), 10 μg/mL BSA (g), and 10 μg/mL γ-globulin (h); (B) reproducibility study of five immunosensors fabricated independently in the presence of 1.0 μg/mL KBL; and (C) stability study of the immunosensor. Error bars represent standard deviation, $n = 3$. Different lowercase letters mean significant differences ($P < 0.05$).

Table 2
Results of immunosensor performance and ELISA in raw and cooked kidney bean milks, n = 3.

Sample	Added (μg/mL)	Found (μg/mL)	Recovery (%)	RSD % (n = 3)	ELISA (μg/mL)
Raw kidney bean milk	0	1.84	–	5.80	2.09
	1.0	2.76	97.18	4.27	2.82
	10.0	10.77	90.96	6.42	10.12
Cooked kidney bean milk	0	0.13	–	8.66	0.25
	1.0	1.08	95.58	7.17	0.97
	10.0	9.83	97.04	2.01	9.85

their initial ΔI after 8 days and 15 days, respectively. Therefore, we concluded that the developed immunosensor presented a good stability during 8 days, which might be ascribed to the good biocompatibility of AuNPs (Yang et al., 2017), high aspect ratio of MWCNTs (Rizwan et al., 2018), and property of PEI to stabilize the nanocomposite layer, as well as SPA to well bind and orient Ab.

3.6. Allergenicity analysis of lectin in real kidney bean milk samples

Although kidney bean-based milks or protein drinks are gaining in popularity (Anino et al., 2019; Chen et al., 2019; Pitura and Arntfield, 2019), the potential allergenicity has attracted extensive attentions because of the activated lectin. In the current research, raw and cooked kidney bean milks were both analyzed by using the developed immunosensor and the conventional ELISA method (Table 2), and 1.84 μg/mL of lectin in raw kidney bean milk (5000 ×) was detected by developed immunosensor, which was close to the reported content of ~10 mg/g seed (Zhang et al., 2008), suggesting a good veracity in practical application. Most notably, the detected lectin content decreased to 0.13 μg/mL (~1/14 of the raw) after cooking (boiled for 30 min), which was consistent with the result of our preliminary experiment. The specific recognition of antibody would be lost, because of the conformational changes of antigenic epitopes during the protein denaturation induced by the heat treatment (Popping et al., 2010). This also implied that cooked kidney bean milks tended to be safer.

Moreover, standard addition method was used to detect the recoveries of different concentrations of KBL in the raw and cooked milk samples. The recovery rate was ranged from 90.96% to 97.18% with the RSD from 2.01% to 8.66%, indicated no systematic error in measurements, even better than similar data observed by the use of amplified ELISA (calibration curve of ELISA shown in Fig. S5), indicating the as-prepared immunosensor had good reliability and accurateness for detection of the allergenic potential in real kidney bean milk samples.

4. Conclusions

In summary, a new-designed label-free voltammetric immunosensor combined with one-pot synthesized AuNPs-PEI-MWCNTs nanocomposite and orientedly Ab immobilization was successfully developed for KBL detection. Compared to other published biosensors, very competitive analytical performances were obtained in our work with wider linear range of 0.05–100 μg/mL and low LOD of 0.023 μg/mL, as well as good selectivity and interference-resistant ability, acceptable reproducibility, and excellent stability. It was noteworthy that a KBL allergenicity-recognition was established in kidney bean milk samples by using the immunosensor. In the future, further nanocomposite synthesis optimization and Ab recognition mechanism investigation would be carried out to enhance the analytical performance of the new-designed immunosensor.

Conflict of interest

The authors declared that they have no conflicts of interest to this

work.

Declaration of competing interest

The authors declare no competing financial interest.

CRediT authorship contribution statement

Xianbao Sun: Formal analysis, Writing - original draft. **Yongkang Ye:** Formal analysis, Writing - original draft. **Shudong He:** Writing - original draft, Formal analysis. **Zeyu Wu:** Formal analysis. **Junyang Yue:** Formal analysis. **Hanju Sun:** Formal analysis. **Xiaodong Cao:** Writing - original draft.

Acknowledgements

The authors are grateful for the financial supports from the National Natural Science Foundation of China (No. 31701524, No. 31772099), the Natural Science Foundation of Anhui Province (No. 1708085MC70, No. 1908085MC98), the Fundamental Research Funds for the Central Universities (No. JZ2018HGTB0245, No. JZ2019YYPY0295), the Financial Grants from China Postdoctoral Science Foundation (No. 2016M592050, No. 2017T100446, No. 2017M611208, No. 2018T110211), and the Anhui Key Research and Development Program (No. 201904a06020030).

Appendix A. Supplementary data

Supplementary data to this article can be found online at https://doi.org/10.1016/j.bios.2019.111607.

References

Abrahmsén, L., Moks, T., Nilsson, B., Hellman, U., Uhlén, M., 1985. EMBO J. 4 (13B), 3901–3906.
Adar, R., Richardson, M., Lis, H., Sharon, N., 1989. FEBS Lett. 257 (1), 81–85.
Afkhami, A., Hashemi, P., Bagheri, H., Salimian, J., Ahmadi, A., Madrakian, T., 2017. Biosens. Bioelectron. 93, 124–131.
Anino, C., Onyango, A.N., Imathiu, S., Maina, J., Onyangore, F., 2019. J. Food Meas. Charact. 13 (2), 1242–1249.
Casas-Solvas, J.M., Ortiz-Salmerón, E., García-Fuentes, L., Vargas-Berenguel, A., 2008. Org. Biomol. Chem. 6 (22), 4230–4235.
Chen, Y.H., Zhang, H., Liu, R.H., Mats, L., Zhu, H.H., Pauls, K.P., Deng, Z.Y., Tsao, R., 2019. J. Funct. Foods 53, 125–135.
Cao, X.Y., Chen, J.J., Wen, S.H., Peng, C., Shen, M.W., Shi, X.Y., 2011. Nanoscale 3 (4), 1741–1747.
Crumbliss, A.L., Perine, S.C., Stonehuerner, J., Tubergen, K.R., Zhao, J.G., Henkens, R.W., O'Daly, J.P., 1992. Biotechnol. Bioeng. 40 (4), 483–490.
Dorval, G., Welsh, K.I., Wigzell, H., 1974. Scand. J. Immunol. 3 (4), 405–411.
Eissa, S., Tlili, C., L'Hocine, L., Zourob, M., 2012. Biosens. Bioelectron. 38 (1), 308–313.
Ey, P.L., Prowse, S.J., Jenkin, C.R., 1978. Immunochem. 15 (7), 429–436.
Haghshenas, E., Madrakian, T., Afkhami, A., Nabiabad, H.S., 2017. Anal. Bioanal. Chem. 409 (22), 5269–5278.
Hatakeyama, T., Murakami, K., Miyamoto, Y., Yamasaki, N., 1996. Anal. Biochem. 237 (2), 188–192.
He, S.D., Shi, J., Li, X.S., Ying, M., Xue, S.J., 2015. LWT - Food Sci. Technol. 60 (2), 1074–1079.
He, S.D., Simpson, B.K., Sun, H.J., Ngadi, M.O., Ma, Y., Huang, T., 2018. Crit. Rev. Food Sci. Nutr. 58 (1), 70–83.
Hu, X.G., Wang, T., Qu, X.H., Dong, S.J., 2006. J. Phys. Chem. B 110 (2), 853–857.
Huang, C.F., Yao, G.H., Liang, R.P., Qiu, J.D., 2013. Biosens. Bioelectron. 50, 305–310.
Huang, K.J., Niu, D.J., Xie, W.Z., Wang, W., 2010. Anal. Chim. Acta 659 (1–2), 102–108.
Jie, Z., Du, L.P., Zou, L., Zou, Y.C., Hu, N., Wang, P., 2014. Sensor. Actuat. B Chem. 197, 220–227.
Jin, L.Y., Gao, X., Wang, L.S., Wu, Q., Chen, Z.C., Lin, X.F., 2013. J. Electroanal. Chem. 692, 1–8.
Kausaite-Minkstimiene, A., Ramanaviciene, A., Kirlyte, J., Ramanavicius, A., 2010. Anal. Chem. 82 (15), 6401–6408.
Kumar, S., Verma, A.K., Das, M., Jain, S.K., Dwivedi, P.D., 2013. Nutrition 29 (6), 821–827.
Kwon, J., Ahn, K.S., Jeong, D., Choi, H.N., Lee, W.Y., 2018. Anal. Lett. 51 (13), 2114–2127.
Li, J.B., Wang, Y.H., Sun, Y.L., Ding, C.F., Lin, Y., Sun, W.Y., Luo, C.N., 2017. RSC Adv. 7 (4), 2315–2322.
Lim, K.R., Ahn, K.S., Lee, W.Y., 2012. Anal. Methods 5 (1), 64–67.
Liu, N., Nie, D.X., Tan, Y.L., Zhao, Z.Y., Liao, Y.C., Wang, H., Sun, C.P., Wu, A.B., 2017. Microchim. Acta 184 (1), 147–153.
Liu, Z.P., Liu, H., Wang, L., Su, X.G., 2016. Anal. Chim. Acta 932, 88–97.
Loaiza, O.A., Lamas-Ardisana, P.J., Jubete, E., Ochoteco, E., Loinaz, I., Cabañero, G., García, I., Penadés, S., 2011. Anal. Chem. 83 (8), 2987–2995.
Malvano, F., Albanese, D., Pilloton, R., Matteo, M.D., 2016. Food Chem. 212, 688–694.
Matucci, A., Veneri, G., Pellegrina, C.D., Zoccatelli, G., Vincenzi, S., Chignola, R., Peruffo, A.D.B., Rizzi, C., 2004. Food Control 15 (5), 391–395.
Miller, T.J., Stone, H.O., 1978. J. Immunol. Methods 24 (1–2), 111–125.
Min, I.H., Choi, L., Ahn, K.S., Kim, B.K., Bo, Y.L., Kim, K.S., Choi, H.N., Lee, W.Y., 2010. Biosens. Bioelectron. 26 (4), 1326–1331.
Miyake, K., Tanaka, T., McNeil, P.L., 2007. PLoS One 2 (8), e687.
Moks, T., Abrahmsén, L., Nilsson, B., Hellman, U., Sjöquist, J., Uhlén, M., 1986. Eur. J. Biochem. 156 (3), 637–643.
Muñoz, E., Suh, D.S., Collins, S., Selvidge, M., Dalton, A.B., Kim, B.G., Razal, J.M., Ussery, G., Rinzler, A.G., Martinez, M.T., Baughman, R.H., 2005. Adv. Mater. 17 (8), 1064–1067.
Ogawa, H., Date, K., 2014. "The "White Kidney Bean Incident" in Japan."//Lectins. Humana Press, New York, pp. 39–45.
Pitura, K., Arntfield, S.D., 2019. Food Chem. 272, 26–32.
Popping, B., Diaz-Amigo, C., Hoenicke, K., 2010. Molecular Biological and Immunological Techniques and Applications for Food Chemists, first ed. John Wiley & Sons, Inc, New Jersey, pp. 492.
Rizwan, M., Elma, S., Lim, S.A., Ahmed, M.U., 2018. Biosens. Bioelectron. 107, 211–217.
Skottrup, P.D., Nicolaisen, M., Justesen, A.F., 2008. Biosens. Bioelectron. 24 (3), 339–348.
Singh, A.C., Bacher, G., Bhand, S., 2017. Electrochim. Acta 232, 30–37.
Simone, V., Gianni, Z., Fabio, P., Corrado, R., Roberto, C., Andrea, C., Peruffo, A.D.B., 2002. J. Agric. Food Chem. 50, 6266–6270.
Sun, Y.F., Liu, J.M., Huang, Y.T., Li, M.M., Lu, J., Jin, N., He, Y., Fan, B., 2019. Int. J. Food Prop. 22 (1), 405–413.
Szunerits, S., Niedziółka-Jönsson, J., Boukherroub, R., Woisel, P., Baumann, J.S., Siriwardena, A., 2010. Anal. Chem. 82 (19), 8203–8210.
Tang, D.Q., Zhang, D.J., Tang, D.Y., Ai, H., 2006. J. Immunol. Methods 316 (1–2), 144–152.
Uslu, B., Ozkan, S.A., 2007. Comb. Chem. High Scr. 10 (7), 495–513.
Vasconcelos, I.M., Oliveira, J.T.A., 2004. Toxicon 44 (4), 385–403.
Vincenzi, S., Zoccatelli, G., Perbellini, F., Rizzi, C., Chignola, R., Curioni, A., Peruffo, A.D.B., 2002. J. Agric. Food Chem. 50 (22), 6266–6270.
Wu, J., He, J.L., Zhang, Y.C., Zhao, Y.L., Niu, Y.Z., Yu, C., 2017. Microchim. Acta 184 (6), 1837–1845.
Yang, L., Zhao, H., Fan, S.M., Deng, S.S., Lv, Q., Lin, J., Li, C.-P., 2014. Biosens. Bioelectron. 57, 199–206.
Yang, Y.Y., Liu, Q., Liu, Y., Cui, J.J., Liu, H., Wang, P., Li, Y.Y., Chen, L., Zhao, Z.D., Dong, Y.H., 2017. Biosens. Bioelectron. 90, 31–38.
Ye, Y.Y., Liu, Y.Q., He, S.D., Xu, X., Cao, X.D., Ye, Y.W., Zheng, H.S., 2018. Sensor. Actuat. B Chem. 272, 53–59.
Ye, Y.Y., Yan, W.W., Liu, Y.Q., He, S.D., Cao, X.D., Xu, X., Zheng, H.S., Gunasekaran, S., 2019. Anal. Chim. Acta 1074, 80–88.
Yu, S.J., Wei, Q., Du, B., Wu, D., Li, H., Yan, L.G., Ma, H.M., Zhang, Y., 2013. Biosens. Bioelectron. 48, 224–229.
Yuan, D.Y., Chen, S.H., Yuan, R., Zhang, J.J., Liu, X.F., 2014. Sensor. Actuat. B Chem. 191, 415–420.
Zeng, H.J., Yu, J.S., Jiang, Y.D., Zeng, X.Q., 2014. Biosens. Bioelectron. 55, 157–161.
Zhao, J.L., He, S.D., Tang, M.M., Sun, X.B., Zhang, Z.Y., Ye, Y.K., Cao, X.D., Sun, H., 2019. J. Food Chem. 283, 183–190.
Zhang, J.S., Shi, J., Ilic, S., Xue, S.J., Kakuda, Y., 2008. Food Rev. Int. 25 (1), 12–27.